Tagged particle motion in a dense liquid: Feedback effects from the collective dynamics

Charanbir Kaur and Shankar P. Das
School of Physical Sciences, Jawaharlal Nehru University, New Delhi 110067, India
(Received 13 January 2003; revised manuscript received 21 March 2003; published 23 May 2003)

The nature of the tagged particle motion in the strongly correlated state of a dense liquid is studied with the self-consistent mode-coupling model. The tagged particle time correlation function $\psi_s(q,t)$ is computed by taking into account the nonlinear feedback effects on its dynamics from the coupling with density fluctuations. We consider the two cases where (a) the short-time dynamics is diffusive resembling colloidal system and (b) the short-time dynamics is Newtonian as in an atomic system. The non-Gaussian parameter $\alpha_2(t)$ is evaluated using the fourth- and second-order spatial moments of the van Hove self-correlation function $G_s(r,t)$. We observe a two-peaked structure of $\alpha_2(t)$ for *both* (a) and (b) types of dynamics. We also compare other characteristic aspects of tagged particle dynamics such as the mean square displacement, non-Gaussian nature of $G_s(r,t)$, and fraction of mobile particles. A qualitative comparison is drawn between the theoretical results with the experimental and computer simulation results on colloids.

DOI: 10.1103/PhysRevE.67.051505 PACS number(s): 64.70.Pf, 05.60.−k, 64.60.Cn

I. INTRODUCTION

The intriguing relaxation features of the various dynamic correlation functions characterizing the dense liquid state have posed active research grounds in recent years. To resolve the underlying mechanisms responsible for the nonexponential relaxations, there has been an upsurge of research activity to correlate the structural and dynamical heterogeneities in a supercooled system. This has been primarily based upon the experimental observations [1–6] and the analysis of the computer simulated many-body dynamics [7–12]. In such studies, the nonexponential relaxation characterizing the supercooled liquids has been often linked to dynamically correlated regions in the system. The heterogeneous distribution of the relatively mobile and immobile regions has also been found to be responsible for the violation of the Stokes Einstein law in fragile glass formers [13]. In Ref. [14], the dynamical heterogeneities were shown to be directly responsible for the decoupling of relaxation and diffusion mechanisms in a supercooled system. This was done through an analysis of the four-point correlation functions obtained from the computer simulation data of the binary Lennard Jones systems. A purely theoretical approach was used in Ref. [15] as a link to understand the origin of the characteristic nonexponential relaxation in a realistic framework of mode-coupling theory (MCT). Various aspects of dense liquid dynamics, especially with respect to the existence of dynamical heterogeneities for a hard-sphere system were presented there. Two different time regimes where the heterogeneous dynamics manifest the most, emerged from this study [15]. The computer simulation of colloidal system [12] also depicted such a two-peak structure of the dynamical heterogeneity parameter. The shorter of these time scales was found to be independent of density variation and was analogous to the results of low-density fluids obtained using the kinetic theory models [16–18]. This represented the effects of correlated dynamics in the initial stages of relaxation in a many-body system.

In the present work, we make an extension of this theoretical approach to study similar aspects in the systems evolving via the Brownian dynamics. Here we refer to a system as (a) ''colloidal'' in which the tagged particle dynamics in the short-time is diffusive and (b) ''atomic'' in which the short-time behavior corresponds to phononlike oscillatory modes. The atomic systems consist of the usual microscopic particles and a colloidal suspension comprises of mesoscopic particles, i.e., much larger sized, suspended in a medium of microscopic particles. Due to the large size difference between the colloid and the solvent particles, there is a complete separation of the relaxation time scales. This results in a ''free'' diffusive motion of the colloid particle in the short-time regime, till it starts interacting with other such particles and the dynamic correlations start building up [19]. A relevant question in the analysis of the dynamics is, how the nature of microscopic dynamics in a system affect the various relaxation mechanisms in a supercooled liquid. Extensive light-scattering experiments on sterically stabilized colloids [20,21] and computer simulation of stochastic dynamics for binary charged colloidal systems in the supercooled state [12,22] have been conducted in this context. Direct comparison of the corresponding relaxations in colloidal and atomic systems have also been conducted numerically using the stochastic and molecular dynamics simulations [23,24]. Most of such studies have been directed specifically toward evaluating the correlation functions and testing whether there is any universality in the asymptotic dynamics irrespective of the nature of microscopic dynamics. The general conclusion being drawn [23,24] is that the microscopic dynamics mainly determines the early β relaxation regime. The atomic systems are characterized by phonon excitations in the initial time range that leads to a faster decay of the correlations as compared to the relaxation in the colloids during the same time range. The α relaxation has been found to be similar in both the systems as regards the stretching exponent [23,24], however, the relaxation time of the atomic system is, in general, smaller than that of the corresponding colloidal system.

In the present paper, we use the self-consistent MCT to theoretically evaluate the comparative nature of correlated dynamics in dense colloidal and atomic systems. This is done

here especially to determine the dynamical heterogeneities that characterize the higher-order cooperative effects of dynamics. The self-consistent MCT has been developed [25–27] and used extensively in the last two decades to understand varied dynamical phenomenon typical of an undercooled system. Various characteristic features of the dense liquid state dynamics observed in experimental studies, such as the two-step relaxation process, divergence of relaxation times, are obtained within this theory. This is as a result of the nonlinear feedback mechanism from the coupling of density fluctuations enhancing the viscosity. The collective density correlation function is used to evaluate relaxation of the tagged particle correlation function [28,15]. The standard form of the MCT equations obtained for the atomic systems does not refer to diffusive motion in the short-time limits. However, in a simplified form of the MCT equations, the collective density correlations have the long-time behavior similar to the Brownian dynamics (Ref. [29]), and will be used for colloids in the present work.

In Sec. II, we briefly discuss the definition of the non-Gaussian parameter $\alpha_2(t)$ and how it signifies the higher-order correlation effects. In Sec. III, we describe the standard theoretical framework of self-consistent mode-coupling theory, and the scheme of evaluating $\alpha_2(t)$. Various aspects of the dynamical equations for the colloidal and atomic systems are discussed here. We present the results in Sec. IV where we illustrate the different dynamical properties of tagged particle motion. We analyze the dynamic variation of the mean square displacement as obtained from this model. The non-Gaussian nature of $G_s(r,t)$ is also illustrated and compared with the corresponding Gaussian distribution at the time t_{p2}—corresponding to the peak of $\alpha_2(t)$. Using this treatment, we identify the fraction of ''mobile'' particles [8] at t_{p2}, which indicate the strong departure from Gaussian behavior. A discussion of these results concludes the paper in Sec. V.

II. THE NON-GAUSSIAN PARAMETER

The single-particle dynamics [18] in a fluid is described by the self-part of the van Hove correlation function

$$G_s(|\vec{r}_1-\vec{r}_2|,t)=V\langle\delta(\vec{r}_1-\vec{R}(t))\delta(\vec{r}_2-\vec{R}(0))\rangle, \quad (2.1)$$

where $\vec{R}(t)$ is the position of the tagged particle at time t in a system of volume V. It is a measure of how the nature of spatial correlation of the tagged particle with its initial position evolves with time. When the microscopic dynamics is Newtonian, the very short time scales correspond to the free particle limit. The $G_s(r,t)$ can be evaluated analytically in this limit [18] and is represented by a narrow Gaussian distribution, $G_s(r,t)=(\pi v_0^2 t^2)^{-3/2}\exp[-(r/v_0 t)^2]$, where v_0 is the thermal velocity of the particles. In a colloidal system, the Brownian dynamics lead to a diffusive behavior $[G_s(r,t)\propto\exp(-r^2/2D_0^s t)]$ in the short-time range, D_0^s being the short-time diffusion coefficient. In the very long-time limit, the motion of the tagged particle becomes diffusive, both in the Newtonian and in the Brownian dynamics and the *Gaussian* spatial variation of $G_s(r,t)$ is obtained. However, over the intermediate time ranges, the complex dynamics in the dense supercooled state lead to a deviation of $G_s(r,t)$ from the Gaussian behavior. This deviation is indicative of the corresponding nonexponential time relaxation of the correlation functions and its quantification constitutes an important step toward our understanding of the basic relaxational mechanisms in a dense liquid. In the computer simulation studies, the evaluation of distinct van Hove correlation function [22] has provided novel insights in the cooperative dynamics of supercooled liquids in the intermediate time regimes of relaxation. Donati *et al.* [9] have found regions of stringlike correlated motion in the liquid in these time scales where the deviation from the Gaussian behavior maximizes. Such results point towards the possibility of the structural and dynamical heterogeneities being self-consistently resulting due to the correlated dynamics.

Rahman [7] first defined the non-Gaussian deviations of $G_s(r,t)$ and hence its Fourier transform, $\psi_s(q,t)$, in terms of the parameters $\alpha_2(t)$, $\alpha_3(t)$ as

$$\psi_s(q,t)=e^{-q^2\rho_1(t)}\left[1+\frac{1}{2!}\alpha_2(t)[q^2\rho_1(t)]^2-\frac{1}{3!}[\alpha_2(t)-3\alpha_3(t)][q^2\rho_1(t)]^3-\ldots\right], \quad (2.2)$$

such that the leading term is Gaussian. Here $\alpha_2(t)$ is defined as the non-Gaussian parameter, $\alpha_2(t)=2\rho_2(t)/[\rho_1(t)]^2$ and $\rho_n(t)$ are expressible in terms of the spatial moments of $G_s(r,t)$, defined as $\langle r^{2n}(t)\rangle=\int d\vec{r}\, r^{2n}(t)G_s(r,t)$. For example, the second moment represents $\langle r^2(t)\rangle$ for $n=1$, which is the mean square displacement of the particle from the origin in time t. By comparing this equation with the cumulant expansion of $\psi_s(q,t)$ in q,

$$\psi_s(q,t)=\sum_{n=0}^{\infty}(-1)^n\frac{q^{2n}}{(2n+1)!}\langle r^{2n}\rangle, \quad (2.3)$$

the $\rho_n(t)$ can be expressed in terms of $\langle r^{2n}(t)\rangle$ [18]. Following which, the $\alpha_2(t)$ is expressible in the standard form as

$$\alpha_2(t)=\frac{3\langle r^4(t)\rangle}{5\langle r^2(t)\rangle^2}-1. \quad (2.4)$$

This definition ensures the $\alpha_2(t)$ to vanish in the limit of a Gaussian distribution of $G_s(r,t)$. The presence of higher-order moments in $\alpha_2(t)$ represents cooperative effects in dynamics.

III. THE SELF-CORRELATION FUNCTION

The dynamical evolution of the characteristic correlation functions is obtained here using the self-consistent MCT. The theoretical framework is mainly based on the systems governed by the Newtonian dynamics. In Ref. [29], the stochastic equation for the dynamics of collective density fluctuations were developed in a projector operator formalism. The Smoluchowski operator is used to describe the dynamics and mode-coupling approximations is applied to finally arrive at

the equation in the long-time limit. This equation is same as the corresponding limit of the dynamical equation for density fluctuation in an atomic system. In an analogous treatment, we compute the colloidal dynamics using the long-time limit of the collective and tagged particle dynamical equations for the Newtonian system. We consider these with appropriate identification of the characteristic time scale and short-time transport in both the systems. This treatment correctly produces the short-time diffusive nature of tagged particle motion in a colloidal system.

The standard MCT is mainly formulated in terms of the correlation between the collective density fluctuations in the system. The Fourier transform of the density autocorrelation function normalized with respect to its equal time value is defined as

$$\psi(q,t)=\frac{\langle \delta\rho^*(\vec{q},t)\,\delta\rho(\vec{q},0)\rangle}{\langle \delta\rho^*(\vec{q},0)\,\delta\rho(\vec{q},0)\rangle}, \tag{3.1}$$

where $\vec{q}$ is the wave vector and the density $\rho(\vec{q},t)=\Sigma_{i=1}^{N}e^{i\vec{q}\cdot\vec{R}_i(t)}$, $\vec{R}_i(t)$ being the position of the ith particle at time t. The tagged particle dynamics are determined in terms of the self-correlation function or the incoherent scattering function, given by

$$\psi_s(q,t)=\langle \delta\rho_s(\vec{q},t)\,\delta\rho_s(-\vec{q},t)\rangle, \tag{3.2}$$

where $\rho_s(q,t)=e^{i\vec{q}.\vec{R}_\alpha(t)}$ is the Fourier transform of the tagged particle density. For the atomic system, the $\psi_s(q,t)$ is evaluated as a numerical solution of the second-order integro differential equation [28,30],

$$\ddot{\psi}_s(q,t)+\left(\frac{\tau v_0}{\sigma}\right)^2\left[q^2\psi_s(q,t)+\mu^{-1}\dot{\psi}_s(q,t)+\int_0^t d\tau'\,\Gamma_s^{mc}(q,t-\tau')\,\dot{\psi}_s(q,\tau')\right]=0. \tag{3.3}$$

Here, v_0 is the average thermal speed of the particles, wave vectors are expressed in dimensionless form ($q\equiv q\sigma$) where the unit of length is the hard-sphere diameter σ, and time is expressed in units of τ. We define τ such that a direct comparison of the Newtonian dynamics with that of the colloidal system can be illustrated. The time scale of relaxation in colloids is usually measured [21,31] in terms of the short-time diffusion coefficient D_0^s, as $\tau=\sigma^2\mu/D_0^s$ with μ being a constant. In order to compare with the experimental results we define $\mu=1/24$ as in Ref. [21]. In the case of the atomic system, we obtain Eq. (3.3) by identifying the short-time diffusion in terms of the bare transport coefficient Γ_s^B, as $D_0^s=v_0^2/\Gamma_s^B$. From the Enskog kinetic theory, the Bare-part Γ_s^B for the hard-sphere Newtonian dynamics is given by $\Gamma_s^B=2/3$ in units of inverse Enskog collision time $t_E=1/[4\sqrt{\pi}g(\sigma)nv_0\sigma^2]$, where n is the average number density and $g(\sigma)$ is the contact value of the radial distribution function.

The mode-coupling contribution $\Gamma_s^{mc}(q,t)$ in Eq. (3.3) takes into account the effect of coupling between the collective and the tagged particle motion. It is expressed in units of v_0^2/σ^2 as

$$\Gamma_s^{mc}(q,t)=\frac{1}{n^*}\int\frac{d\vec{k}}{(2\pi)^3}\psi_s(|\vec{q}-\vec{k}|,t)V_s(\vec{q},\vec{k})\psi(k,t). \tag{3.4}$$

Here the vertex function is obtained in terms of the static fluid properties as [28] $V_s(\vec{q},\vec{k})=(\hat{q}.\vec{k})^2[\tilde{c}(k)]^2S(k)$. The average number density of the liquid is expressed here in dimensionless form as $n^*=n\sigma^3$. The static structure factor is denoted as $S(k)$ and $\tilde{c}(k)=nc(k)$, $c(k)$ being the Ornstein-Zernike direct correlation function.

In the long-time limit, the second derivative term is ignored in Eq. (3.3) to obtain

$$\dot{\psi}_s(q,t)+\mu\left[q^2\psi_s(q,t)+\int_0^t d\tau'\,\Gamma_{mc}^s(q,t-\tau')\,\dot{\psi}_s(q,\tau')\right]=0. \tag{3.5}$$

This shows a diffusive relaxation for $\psi_s(q,t)$ in the short-time limit as expected for a colloidal system. Therefore, we will consider this equation for computing the tagged particle dynamics for this system. In Eq. (3.5), as mentioned above the unit of time τ is identified with respect to the short-time diffusion coefficient D_0^s. This time scale τ is generally measured in the light-scattering studies of colloids [21] ($\tau\sim 0.0215$ sec).

The dynamical evolution of $\psi_s(q,t)$ is coupled with the corresponding relaxation of the collective density fluctuations $\psi(q,t)$, through the mode-coupling kernel $\Gamma_s^{mc}(q,t)$ [Eq. (3.4)]. We use the extended mode-coupling model [26] for obtaining this crucial input to the theory. The Laplace transformed equation governing the relaxation of $\psi(q,t)$ in this model [26] is expressed as

$$\psi(q,z)=\frac{z+i\Gamma^R(q,z)}{z^2-\Omega_q^2+i\Gamma^R(q,z)[z+iq^2\gamma(q,z)]}, \tag{3.6}$$

where $\Omega_q=qv_0/\sqrt{S(q)}$ corresponds to a characteristic microscopic frequency for the liquid state dynamics and $\Gamma^R(q,z)$ is the renormalized longitudinal viscosity. This is obtained using nonlinear fluctuating hydrodynamics by an appropriate treatment of the nonlinear coupling between current and density fluctuations characterizing a compressible fluid [26,27]. The memory function

$$\Gamma^R(q,z)=\Gamma_B(q)+\int_0^\infty dt\Gamma_{mc}(q,t)e^{izt}, \tag{3.7}$$

where $\Gamma_B(q)$ is the Bare part or the contribution due to the initial uncorrelated collisions in the liquid. The mode-coupling part $\Gamma_{mc}(q,t)$ accounts for the memory effects due to the correlated motion in the dense liquid, which become significant over intermediate and long time scales. It is obtained within the one-loop approximation [26,32] as a bilinear coupling between the density fluctuations [32],

$$\Gamma_{mc}(q,t)=\frac{1}{2n^*q^2}\int \frac{d\vec{k}}{(2\pi)^3}\psi(k,t)V(\vec{q},\vec{k})\psi(|\vec{q}-\vec{k}|,t) \tag{3.8}$$

in units of v_0^2/σ^2, such that a self-consistent equation is obtained for $\psi(q,t)$ from Eq. (3.6). The vertex function in Eq. (3.8),

$$V(\vec{q},\vec{k})=S(k)S(|\vec{q}-\vec{k}|)[(\hat{q}.\vec{k})\tilde{c}(k)-\hat{q}.(\vec{q}-\vec{k})\tilde{c}(|\vec{q}-\vec{k}|)]^2. \tag{3.9}$$

In Eq. (3.6), the function $\gamma(q,z)$ represents the cutoff function that is responsible for keeping the system ergodic at all densities. We use the expression obtained for this function in the one-loop approximation ([27,32]). In the present work, we have used $\gamma(q,t)$ with a factor δ in order to consider the finite wave-vector generalization. This determines the strength of $\gamma(q,t)$ and thus the time scale of α relaxation such that consistency with the experimental results can be obtained by appropriately fixing the single parameter δ. The simple version of the mode-coupling model [25] results if $\gamma(q,z)$ is ignored in Eq. (3.6), or equivalently if one sets $\delta=0$. An ergodic to nonergodic dynamic transition results in the simple model at a critical packing fraction $\varphi_c\approx 0.516$ [25,32] ($\varphi=\pi n^*/6$) where the dynamic correlations freeze at a nonzero value. The molecular dynamics studies [33] and the light-scattering experiments of colloids [20] showed that the dynamics became increasingly slow with density rise. However, the conclusion on the occurrence of a sharp transition is not forthcoming. These light-scattering results [20] were exhaustively analyzed in Ref. [34] within a phenomenological model of the extended MCT [35] to show that even up to the highest density, the relaxation time of the correlation functions remained finite. In the present work, we have considered both the simple and the extended mode-coupling models.

To numerically evaluate the dynamical variation of $\psi_s(q,t)$, we first inverse-Laplace transform Eq. (3.6) to obtain the time evolution of the $\psi(q,t)$ as a second-order integrodifferential equation for the Newtonian dynamics [32]. The Bare contribution to the generalized longitudinal viscosity is obtained from the Enskog kinetic theory as $\Gamma_B(x)=(2/3t_E)[1-j_0(x)+2j_2(x)]$. Here j_l is the spherical Bessel function of order l and $x=q\sigma$. The corresponding equation for the Brownian dynamics is obtained by ignoring the $\ddot{\psi}(q,t)$ term (as similarly done for the self-correlation function) and is explicitly given by

$$\dot{\psi}(q,t)+\mu' q^2\Bigg[\int_0^t d\tau'\Gamma_{mc}(q,t-\tau')\dot{\psi}(q,\tau') + [S(q)]^{-1}\psi(q,t)+\int_0^t d\tau_1\gamma(q,t-\tau_1)\Bigg(\frac{\psi(q,\tau_1)}{\mu'} + \int_0^{\tau_1} d\tau_2\Gamma_{mc}(q,\tau_1-\tau_2)\psi(q,\tau_2)\Bigg)\Bigg]=0. \tag{3.10}$$

The unit of time τ is defined in terms of D_0^s, as described earlier. Here $\mu'=\mu D_0/D_0^s$, where D_0 refers to the short-time transport coefficient identified as $D_0=v_0^2/\Gamma_B$ for the collective density fluctuations of the Brownian dynamics case. In the present work, we have fixed this ratio μ' as 1/24. The experimental studies of colloids show that the static properties like the structure factor $S(k)$ are similar to that of a hard-sphere liquid. Therefore, we use the Percus Yevick solution for $S(k)$ in both the Newtonian and the Brownian system.

A. Evaluation of the non-Gaussian parameter

We evaluate the $\psi_s(q,t)$ in the small wave-vector range, such that it can be equated to the cumulant expansion [Eq. (2.3)] truncated at $O(q^4)$. The second and fourth spatial moments $\langle r^2(t)\rangle$ and $\langle r^4(t)\rangle$, are thus obtained on curve-fitting $[1-\psi_s(q,t)]/q^2$ to a linear form with respect to q^2. The slope is $\frac{1}{6}\langle r^4(t)\rangle$ and the intercept is given by $-\frac{1}{120}\langle r^4(t)\rangle$. From this, we calculate $\alpha_2(t)$ from Eq. (2.4).

To evaluate $\psi_s(q,t)$ in the small q range, the memory function $\Gamma_s^{mc}(q,t)$ is expressed as an expansion in q given by

$$\Gamma_s^{mc}(q,t)=\Gamma_0(t)+q^2\Gamma_2(t)+q^4\Gamma_4(t)+\cdots, \tag{3.11}$$

by using the Taylor series expansions of $\psi_s(|\vec{q}-\vec{k}|,t)$ and $V_s(\vec{q},\vec{k})$ in Eq. (3.4). The coefficients $\Gamma_{2n}(t)$ involve the wave-vector integrals of second- and higher-order q derivatives of $\psi_s(q,t)$ and $\psi(q,t)$. These are given by

$$\Gamma_0(t)=\frac{2}{3}\int dk k^4\tilde{c}^{\,2}(k)S(k)\psi_s(k,t)\psi(k,t) \tag{3.12}$$

and

$$\Gamma_2(t)=\int dk k^4\tilde{c}^{\,2}(k)S(k)\left[\frac{2}{15k}\psi_s'(k,t)+\frac{1}{5}\psi_s''(k,t)\right]\psi(k,t), \tag{3.13}$$

where $\psi_s'(k,t)=(\partial/\partial k)\psi_s(k,t)$. To evaluate $\alpha_2(t)$, the q expansion [Eq. (3.11)] is truncated at $O(q^2)$, i.e., one needs to compute only $\Gamma_0(t)$ and $\Gamma_2(t)$. To calculate the higher-order non-Gaussian effects like $\alpha_3(t)$ will require the quantity $\Gamma_4(t)$ in Eq. (3.11) to be evaluated. This is expressed in terms of even higher-order k derivatives that are difficult to obtain numerically with sufficient accuracy.

In the atomic system characterized by the Newtonian dynamics, the tagged particle moves as a free particle for very short time in a straight line trajectory, and hence its probability of being at a position $\vec{r}$ in time t can be expressed simply as $\delta(\vec{r}-\vec{v}t)$ [18]. Using the Maxwellian distribution for the velocity $\vec{v}$, the $G_s(r,t)$ is obtained as $G_s(r,t)=(\pi v_0^2t^2)^{-3/2}\exp[-(r/v_0t)^2]$. So, in the $t\to 0$ limit, $G_s(r,t)$ is a Gaussian function and $\alpha_2(t)$ should vanish identically in this limit. The correct short-time behavior is $\alpha_2(t)\to 0$ as $\sim t^8$ [16]. The present theoretical model, however, does not produce this short-time limit of $\alpha_2(t)$ and is mainly formulated to take into account the correlated dynamical effects in

dense liquid systems. Dynamical equation (3.3) is obtained [28] within a generalized *hydrodynamic* context. It is not valid for time scales lesser than the average collision time. In the present model, the dynamic equation for the tagged particle momentum density $\vec{g}_s$ would contain a damping term even in the $t\to 0$ limit which is certainly not the free-particle dynamics. On taking the corresponding limit in Eq. (3.3), we find $\alpha_2(t)$ tends towards a negative constant value $-2/3$ as $t\to 0$ [36]. Here, it is worth noting that the evaluation of $\alpha_2(t)$ for the low-density fluids in the kinetic theory approximation [16–18] also does not produce the correct short-time limit. Although these are based on a microscopic treatment of the collision processes, these predict that $\alpha_2(t)\to 0$ as $\sim t$, rather than the correct variation $\sim t^8$ [18]. For the case of the Brownian dynamics, however, in the limit $t\to 0$, Eq. (3.5) reduces to a diffusive equation, hence the $\alpha_2(t)$ vanishes as $t\to 0$.

B. Asymptotic limit of $\alpha_2(t)$ beyond φ_c in simple MCT

The long-time limit of $\alpha_2(t)$ should identically be zero as the tagged particle motion becomes totally diffusive in an ergodic liquid. However, in the simple MCT model [25], an ergodic to nonergodic transition occurs in the system at a critical packing fraction φ_c. This is marked by the freezing of the density and single particle correlations. Thus beyond φ_c, $\psi(q,t)\to f(q)$ and $\psi_s(q,t)\to f_s(q)$ in the dynamic asymptotic limit. The final diffusive relaxation of $\psi_s(q,t)$ that causes $\alpha_2(t)$ to vanish, never occurs beyond φ_c in this model. As a consequence, $\alpha_2(t)$ also becomes a nonzero constant α_2^0, in the long-time limit at densities beyond φ_c.

Evaluation of α_2^0

The self-correlation function can be expressed as $\psi_s(q,t)=f_s(q)+\tilde{\psi}_s(q,t)$ where $\tilde{\psi}_s(q,t)\to 0$, as $t\to\infty$ for $\varphi>\varphi_c$. In this case, the Laplace transform of Eq. (3.3) reduces to

$$f_s(q)=\frac{\Gamma_s^{mc}(q,t\to\infty)}{q^2v_0^2+\Gamma_s^{mc}(q,t\to\infty)}. \tag{3.14}$$

Now in the small q limit, expansion (3.11) is used to approximate $\Gamma_s^{mc}(q,t\to\infty)$ in terms of the asymptotic values of $\Gamma_0(t)$ and $\Gamma_2(t)$. It is important to indicate here that the asymptotic limits of $\Gamma_0(t)$ and $\Gamma_2(t)$ are nonzero constant values for $\varphi>\varphi_c$ in the simple MCT model. By expressing Eq. (3.14) as a q expansion, and equating to cumulant expansion (2.3), the asymptotic spatial moments are obtained as

$$\langle r^2(t\to\infty)\rangle=6\frac{v_0^2}{\sigma^2A_0}, \tag{3.15}$$

$$\langle r^4(t\to\infty)\rangle=120\left[\frac{v_0^2}{A_0\sigma^2}\right]^2\left(1+\frac{A_2}{v_0^2}\right),$$

where A_0 and A_2 are the long-time values of $\Gamma_o(t)$ and $\Gamma_2(t)$, respectively, which are obtained numerically. Using these, the asymptotic value of $\alpha_2(t)$ is evaluated as

$$\alpha_2^0=2\frac{A_2}{v_0^2}+1. \tag{3.16}$$

However, in the extended MCT model, the $\Gamma_s^{mc}(q,t\to\infty)\to 0$ and hence $\alpha_2(t)$ vanishes in the asymptotic limit at all densities. These long-time features of $\alpha_2(t)$ apply identically to both the colloidal and the atomic systems.

IV. RESULTS

We now discuss our results for the various features of tagged particle dynamics in both the cases of Newtonian and Brownian dynamics. We evaluate $\alpha_2(t)$ according to the scheme defined in Sec. III A. We obtain the self-correlation function $\psi_s(q,t)$ for the atomic system as the numerical solution of Eq. (3.3) and that of colloidal system from Eq. (3.5). Before going into the specific features of dynamics in both the cases, we first elaborate on the general results. We find that $\alpha_2(t)$ shows two distinct peaks—one in the short-time β relaxation regime and the other in the long-time α relaxation region [15]. The two-peak structure of non-Gaussian parameter has also been observed in the computer simulation study of a charged colloidal system in Ref. [12]. In the theoretical studies of low-density fluids, kinetic theory models were used to include the higher-order correlation effects [16–18] in the single-particle dynamics. The peak in $\alpha_2(t)$ calculated in these models occurred in the similar time range ($\sim 10t_E$) as observed in our results as the first peak in $\alpha_2(t)$. We find that the position of this peak hardly changes with density variation—a feature that was similarly found in the results obtained in the kinetic theory studies, and also apparent in the results shown in Fig. 16 of Ref. [12]. The second peak occurring in the α relaxation time range is a consequence of longer-ranged correlated dynamical effects in a dense liquid, and thus it is not observed in the lower-density fluids.

In Sec. IV A, we describe the evaluation of $\alpha_2(t)$ in the shorter-time region with the simple MCT model that predicts ideal glass transition. Note that, the simple or extended versions of MCT predict similar short-time behavior. Our results illustrate the significance of including the short wavelength fluctuations in the evaluation of correlated effects over relatively short-time scales. The comparative description of results for the two types of dynamics are presented in Sec. IV B using the extended MCT model.

A. Simple MCT model

The evaluation of $\alpha_2(t)$ in the MCT model involves the numerical calculation of wave-vector integrals. Thus the effect of fixing the upper wave-vector cutoff Λ in such integrals is an important aspect to be considered in order to ascertain the quantitative correctness of results. We conducted a detailed numerical analysis of the above equations

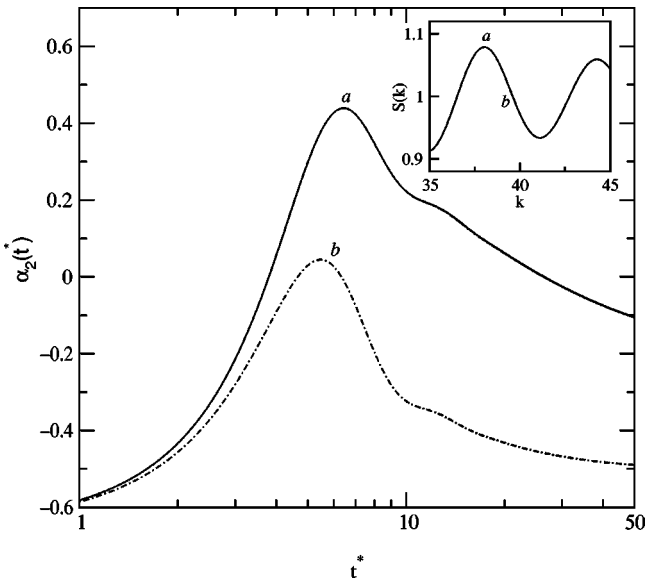

FIG. 1. Non-Gaussian parameter $\alpha_2(t)$ vs $t^*=t/t_E$ for the Newtonian system at $\varphi=0.565$. The inset shows $S(k)$ at $\varphi=0.565$, where the relative locations of Λ values for curves *a* and *b* are indicated.

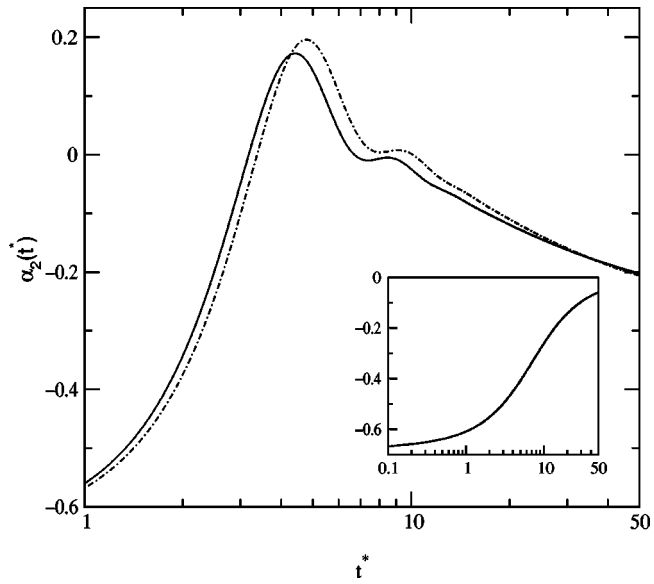

FIG. 2. $\alpha_2(t)$ vs t^* ($t^*=t/t_E$) for the Newtonian system at $\varphi=0.565$. The solid line is obtained with $\Lambda=60\sigma^{-1}$ and the dot-dashed curve is for $50\sigma^{-1}$. The result with the linearized dynamical equation (without the mode coupling term) is shown in the inset at the same φ.

especially in this regard. We separately present below the results for the Newtonian and the Brownian dynamic cases.

In the short and intermediate time regimes, the $\alpha_2(t)$ results show convergence at a large Λ value ($\approx 60\sigma$). With the choice of smaller Λ, however, the qualitative features of $\alpha_2(t)$ as discussed above remains unaltered over the whole time range in the atomic systems. The quantitative dependence on Λ is governed by the fact that whether or not the value of upper cutoff corresponds to an extrema of the static structure factor $S(k)$. For cutoff values corresponding to the maximum or minimum of the $S(k)$, the peak in $\alpha_2(t)$ is comparatively larger. To investigate this feature over the entire time range of different relaxation regimes, we consider a relatively small packing fraction, $\varphi=0.500$ to extract the effects of changing Λ on the long-time behavior of $\alpha_2(t)$. In Fig. 1, we illustrate this feature of $\alpha_2(t)$ for Newtonian dynamics at $\varphi=0.565$ for intermediate time scales. Here Λ lies in the relatively shorter range. Two curves (a) and (b) are evaluated with Λ, respectively, fixed at the maximum and at an intermediate value of $S(k)$, as illustrated in the inset plot of $S(k)$. These results show a convergence with the increase in the Λ finally to a distinct peak at $\Lambda\approx 60\sigma^{-1}$. In the Fig. 2, we illustrate the results for $\Lambda=50\sigma^{-1}$ (dot-dashed) and $\Lambda=60\sigma^{-1}$ (solid) with the distinct short-time peak in $\alpha_2(t)$. These are of the same form as curve (a) shown in Fig. 1. To illustrate the fact that the short-time peak in $\alpha_2(t)$ is a result of the correlated effect of dynamics, we evaluate $\alpha_2(t)$ from the linearized dynamical equation by ignoring the mode-coupling term. The result is shown at same φ in the inset of Fig. 2 that shows a simple monotonically increasing variation towards zero, without any indication of a peak in $\alpha_2(t)$.

These results suggest that since the numerical solution of the dynamical equations involves calculation of oscillatory wave-vector integrals, the upper limit of these should be optimized such that one can ignore further contributions to the integral due to cancellation. Our comparison with the finally converged results shows that fixing Λ at wave vector corresponding to an extremum of $S(k)$ is an optimum choice in this regard. This is important since evaluating $\alpha_2(t)$ up to large time scales numerically with a very large Λ is computationally impractical. The wave-vector grid of size $0.1\sigma^{-1}$ was found to be optimum in terms of convergence of results and has been used in all the calculations reported in the present work. In the simple MCT model used here to evaluate $\alpha_2(t)$, the first peak distinctly shows up even at densities greater than φ_c, at which the correlations are frozen in the long-time regime. In such cases, the long-time peak is not observed and the $\alpha_2(t)$ becomes constant at a nonzero value in $t\rightarrow\infty$, as discussed in Sec. III B.

The variation of $\alpha_2(t)$ is primarily determined from the structure of $\Gamma_2(t)$ [Eq. (3.13)]. In Fig. 3, we illustrate the different curves of $\Gamma_2(t)$ that determined the corresponding $\alpha_2(t)$ in the Fig. 2, for the different Λ values. In the inset of this figure, the normalized value of $\Gamma_0(t)$ [Eq. (3.12)], denoted as $\overline{\Gamma}_0(t)$, is shown which displays a simple monotonic decrease at all Λ values for the whole time variation. The structure of $\Gamma_2(t)$, however, indicates the origin of first peak of $\alpha_2(t)$ as the peak on the same timescale. The initial positive bump in $\Gamma_2(t)$ determines the height of the first peak in the corresponding $\alpha_2(t)$. The convergence of results with increase in Λ is also apparent from this figure.

The second or the larger time peak in $\alpha_2(t)$ shows comparatively less variation with respect to change in Λ, since in the longer-time regimes, the major contribution in the wave-vector integrals is from the k ranges corresponding to the structure factor maximum. Figure 4 highlights this aspect of the non-Gaussian parameter where the $\alpha_2(t)$ variation for the Newtonian dynamics is illustrated up to larger time

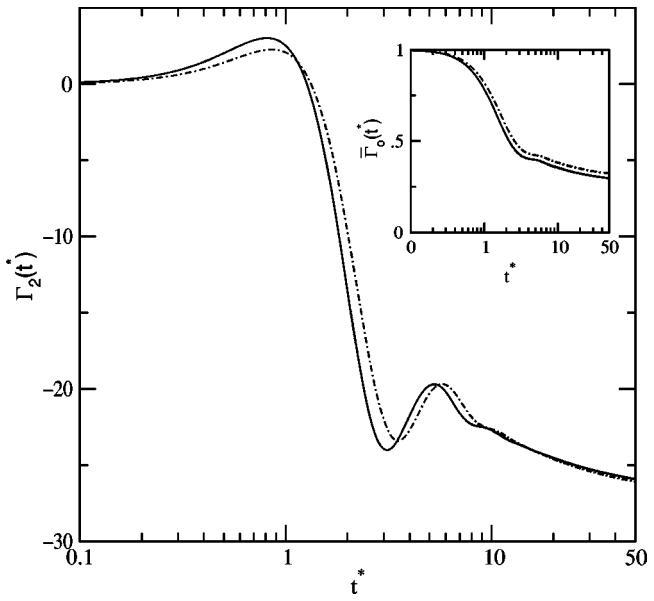

FIG. 3. Variation of $\Gamma_2(t)$ (in units of v_0^2) with t^* for the Newtonian system at $\varphi=0.565$. The solid line is obtained with $\Lambda=60\sigma^{-1}$ and the dot-dashed curve for $50\sigma^{-1}$. The normalized $\bar{\Gamma}_0(t)$ (dimensionless) is illustrated in the inset.

scales for $\varphi=0.500$, using the simple MCT model. The three curves are evaluated using different values of Λ corresponding to the k value of the successive maximum, intermediate, and minimum of the $S(k)$, respectively. The shape and height of the second peak remains almost invariant due to the Λ variation, however, the position of the peak shifts to larger time scales with increase in Λ.

The features of the present model described above apply almost identically to the case of the Brownian dynamics. We observe a similar two-peaked structure of the non-Gaussian

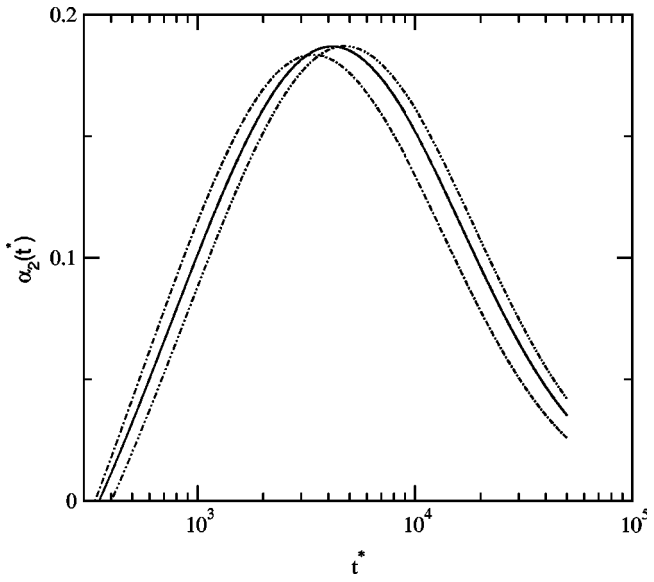

FIG. 4. Long-time peak in $\alpha_2(t)$ vs t^* for the Newtonian system at $\varphi=0.500$ for $\Lambda=30.0$ (dotted), 34.5 (solid), and 38.0 (dot-dashed).

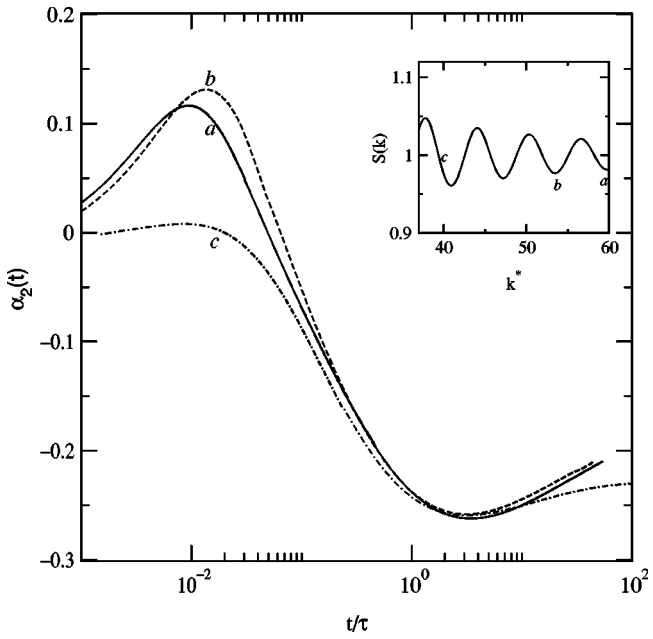

FIG. 5. Non-Gaussian parameter $\alpha_2(t)$ vs t in units of τ for the system following the Brownian dynamics at $\varphi=0.516$. The results are shown with respect to different Λ values indicated as a,b,c in the curve of $S(k)$ as shown in the inset.

parameter. However, if Λ has a value which is intermediate between two extrema of $S(k)$, the short-time peak is hardly observable. Thus, for example, $\Lambda\sigma=39.8$ [37] does not corresponds to an extrema of $S(k)$ and so the first peak is not observed in this case. In Fig. 5, we illustrate the variation of $\alpha_2(t)$ for the colloidal system with different choices for Λ. The relative location of the corresponding cut-off values with respect to the extrema of $S(k)$ are shown as an inset of Fig. 5. These results are obtained using the simple MCT model for stochastic dynamics at $\varphi=0.516$. Here we clearly observe that curve c is computed with Λ located in between the extrema and no peak in $\alpha_2(t)$ appears in this case [37].

B. Extended MCT Results

The simple version of MCT predicts zero diffusivity even at densities as low as $\varphi_c=0.516$ [25], contradicted by the computer simulation results [33]. In this model, for atomic [15] as well as for colloidal systems [37] the long-time peak in the non-Gaussian parameter is not observable for densities beyond φ_c, instead it freezes to a constant value (Sec. III B). In contrast, the light-scattering experiments on colloids show a strong peak in $\alpha_2(t)$ at densities as high as $\varphi=0.572$ (Ref. [31]). This limitation of simple MCT model is overcome by the use of the extended MCT discussed in Sec. III. In Ref. [15] as well, the main aspects of tagged particle dynamics in the atomic system were considered using this model. For the colloidal system, we evaluate the non-Gaussian parameter at $\varphi=0.542$ by using the extended model equations for the Brownian dynamics [Eq. (3.5) and Eq. (3.10)]. We adjust the parameter δ such that the relaxation time τ_α characterizing the stretched exponential-α relaxation regime of $\psi(q,t)$, is identical to that of the corresponding data obtained by the

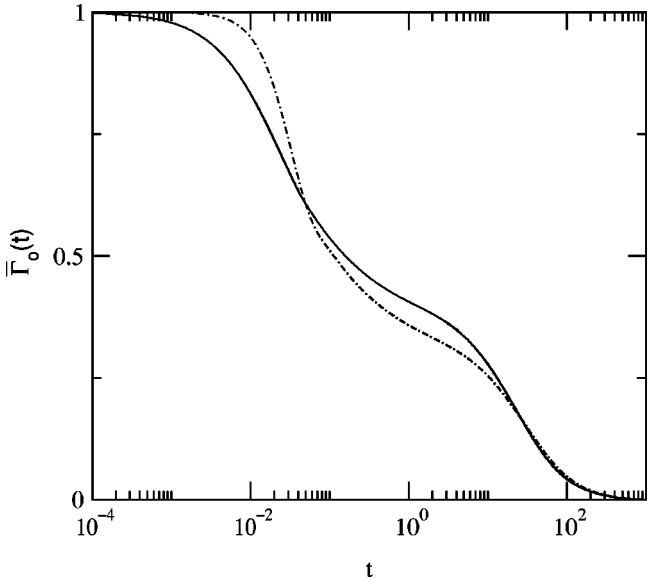

FIG. 6. Comparison of the different relaxation regimes of normalized memory function $\bar{\Gamma}_0(t)$ for the Brownian (solid line) and the Newtonian (dot-dashed line) systems at $\varphi=0.542$. The time $t \equiv t/\tau$.

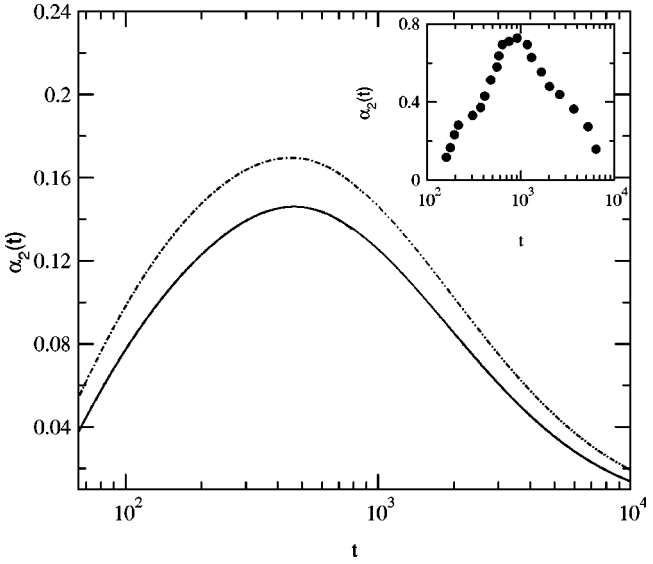

FIG. 7. The Long-time peak in $\alpha_2(t)$ ($t \equiv t/\tau$), compared for the Newtonian (dot-dashed line) and Brownian (solid line) system at $\varphi=0.542$ using the extended MCT. The inset shows the corresponding $\alpha_2(t)$ obtained experimentally in Ref. [31] at $\varphi=0.540$.

light scattering experiments on colloids [Fig. 5(a) of Ref. [20]). This matching is done at the wave vector corresponding to the peak of structure factor. With this criterion, our results show a faster rate of relaxation as compared to the experimental results although the overall time scales of relaxation match. The stretching exponent β is higher than that obtained in the experimental results by about 12%. For direct comparison, we evaluate the Newtonian dynamics at the same packing fraction φ and the parameter δ as used for calculating the dynamics of the colloid. The Λ in this calculation is fixed at $25\sigma^{-1}$ as we will be mainly discussing the long-time features. The different relaxation regimes of the normalized memory function $\bar{\Gamma}_0(q=0,t)$ for $\psi_s(q,t)$ [Eq. (3.12)] are shown in Fig. 6. In the early β relaxation regime, the slow dynamics of the colloidal system (solid line) is observed as compared to the faster relaxation of the Newtonian system (dot-dashed line). During the latter α relaxation range, both the systems show similar variation. These features are also observed in the computer simulation studies reported in Refs. [23,24] where comparative studies of Newtonian and stochastic dynamics in a supercooled system were made.

1. Non-Gaussian parameter

We evaluate $\alpha_2(t)$ for both the systems using the method outlined in Sec. III A. These results are shown in the Fig. 7, where we illustrate the Brownian dynamical results by the solid line and $\alpha_2(t)$ for the Newtonian system as the dot-dashed curve. $\alpha_2(t)$ show the maximum at the same time for both the systems, although the heights of the two peaks are slightly different at this time. The higher-order moments of $G_s(r,t)$ determining $\alpha_2(t)$ are susceptible to changes even due to a slight difference of the relaxation in the correlation. In the longer-time region, these two curves show a converging trend. The results of $\alpha_2(t)$ obtained in the experimental studies of colloidal suspensions at a slightly lower density $\varphi=0.540$ [31] appears at $\approx 800\tau$, which is of the same order as obtained in our results of Fig. 7 ($\approx 400\tau$). The inset shows the $\alpha_2(t)$ obtained from the light-scattering experiments reported in Ref. [31]. The peak height of $\alpha_2(t)$ obtained from the theoretical calculation is much lower than that obtained in the experimental data. The theoretical curves are obtained with only a *single* adjustable parameter δ that was chosen so as to match the time scale of relaxation of $\psi(q,t)$ with the experimentally obtained results [20], at a single q value. Comparison with $\alpha_2(t)$ obtained from the light-scattering studies at the highest density $\varphi=0.570$ [31] has not been shown here since that will involve further computational effort by almost another three orders of magnitude. The density dependence of $\alpha_2(t)$ obtained in the present theoretical model is further illustrated in Fig. 8. Here we show $\alpha_2(t)$ for the atomic system corresponding to three different packing fractions φ. These results are obtained using the extended MCT model with δ kept fixed at a value so as to match the theoretically obtained self-diffusion coefficient at $\varphi=0.565$ [15], with that obtained from computer simulations of one-component hard-sphere systems as reported in Ref. [33]. $\alpha_2(t)$ shows an increasing deviation from the Gaussian behavior and the approach towards the maximum deviation becomes slower with an increase in density. These qualitative features have also been observed in the molecular dynamics simulation of two-component systems with different interaction potentials [8,38]. We show a qualitative comparison of our results with $\alpha_2(t)$ for the binary Lennard Jones (LJ) system in the inset of Fig. 8. These data are taken from the results shown in Fig. 1 of Ref. [8].

In Fig. 9, we have shown the conditional probability distribution function $4\pi r^2 G_s(r,t)$ in both the Newtonian and the Brownian systems at the time where the second peak in

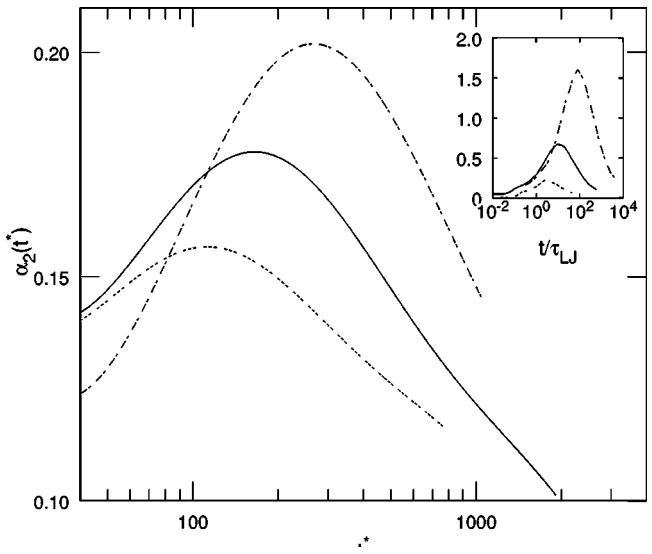

FIG. 8. Comparison of the $\alpha_2(t)$ variation at different densities for the Newtonian system. The dashed line shows $\alpha_2(t)$ at $\varphi = 0.550$, the solid line is for $\varphi = 0.565$, and the dot-dashed curve is for $\varphi = 0.570$. The dimensionless time $t^* = t/t_E$, t_E being the Enskog collision time. The inset illustrates the result from Ref. [8] for a binary LJ system at temperatures $T^* = 0.550$ (dashed), $T^* = 0.480$ (solid), and $T^* = 0.451$ (dot-dashed). Here T^* is the reduced temperature in LJ units ($T^* = k_B T/\epsilon_{AA}$) and time is expressed in the LJ time scale $\tau_{LJ} = \sqrt{\sigma_{AA}^2 m/\epsilon_{AA}}$ [8].

$\alpha_2(t)$ appears (Fig. 7). $G_s(r,t)$ of both the systems at this time are practically indistinguishable from each other and thus illustrates again the similarity of dynamics in both systems in the later relaxational time range. Here, we have

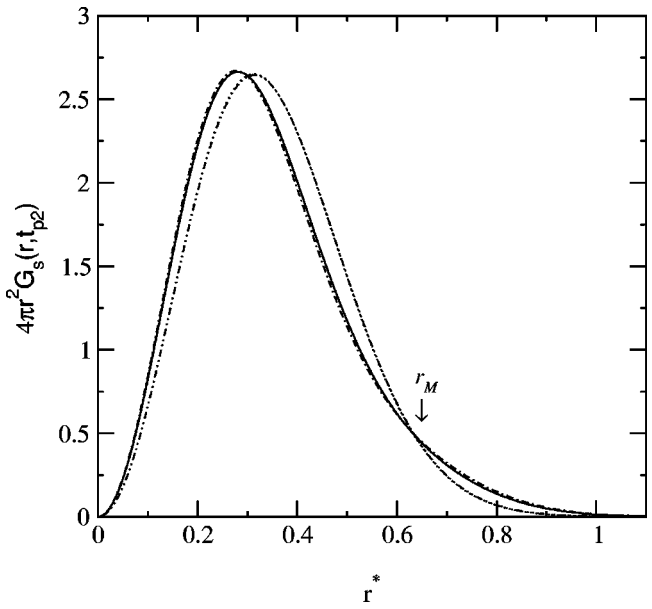

FIG. 9. $4\pi r^2 G_s(r,t)$ vs $r^* = r/\sigma$ for the two systems at $\varphi = 0.542$ compared with the corresponding Gaussian distribution shown as the double dot-dashed line. t_{p2} is the time (in units of τ) at which $\alpha_2(t)$ shows the long-time peak in Fig. 7. The respective curves of the Newtonian and the Brownian systems are almost indistinguishable.

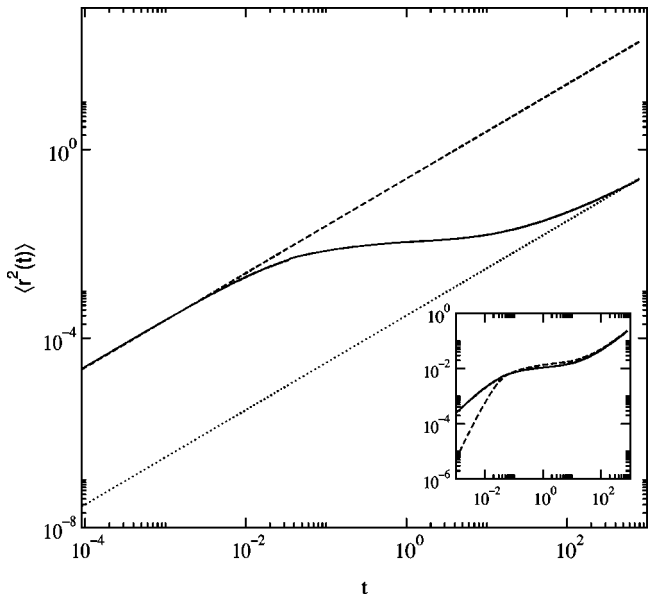

FIG. 10. Mean square displacement $\langle r^2(t)\rangle$ (in units of σ^2) vs time $t \equiv t/\tau$ for the Brownian system at $\varphi = 0.542$. Dashed and dotted lines show the short- and the long-time diffusive motion, respectively. The inset shows the comparison for the Newtonian (dashed) and the Brownian (solid) systems at the same φ.

shown the comparison of this function with the corresponding Gaussian distribution $G_s^0(r,t) = [3/(2\pi\langle r^2(t)\rangle)]^{3/2} \exp[-3r^2/2\langle r^2(t)\rangle]$ by using $\langle r^2(t)\rangle$ at the position of the long-time peak in $\alpha_2(t)$. This is illustrated as the double dot-dashed line in this figure. Beyond the distance r_M (marked in the Fig. 9 by the arrow), $G_s(r,t)$ develops a slowly decaying tail, and thus the probability of finding the tagged particle is greater than that predicted by the corresponding $G_s^0(r,t)$. In the computer simulation studies of Kob *et al.* [8], the particles that crossed the distance r_M were labeled as "mobile" particles. Such highly correlated clusters of particles lead to a heterogeneous distribution of mobile and relatively immobile regions in the system that pertain to have different relaxation rates. In the present case, the fraction of "mobile" particles evaluated as $\int_{r_M}^{\infty} dr\ 4\pi r^2 G_s(r,t)$ is the same in both the cases.

2. Mean square displacement

The mean square displacement is the second moment of $G_s(r,t)$. The initial variation of $\langle r^2(t)\rangle$ in a Brownian system is diffusive ($\langle r^2(t)\rangle \propto t$) and is ballistic ($\langle r^2(t)\rangle \propto t^2$) in the Newtonian dynamics. The time variation of the mean square displacement $\langle r^2(t)\rangle$ is a strong indicator of the interplay between the collective and the tagged particle dynamics in dense liquid state. We show in Fig. 10, the crossover from short-time diffusion to long-time diffusive behavior in the Brownian dynamics case. The intercepts of the curve show the comparative decrease in diffusion coefficients. In the inset of Fig. 10, we have compared the time evolution of $\langle r^2(t)\rangle$ for the Brownian (solid) and the Newtonian (dot-dashed) dynamics. The different increasing rates of $\langle r^2(t)\rangle$ are evident from this figure, shown in a log-log

plot. Over intermediate times, a plateaulike region appears which demonstrates the so-called cage effect during which the tagged particle is trapped in a cage formed due to the collective motion of the surrounding particles. This is observed in both the types of dynamics and corresponds to the late β relaxation regime. With progress of time, the particle comes out of the cage and shows a subdiffusive behavior ($\langle r^2(t)\rangle \propto t^a, a<1$). Finally, its motion becomes purely diffusive ($a=1$) in the very long-time regime. Stronger the jamming of the supercooled liquid is, slower is these crossover process and hence the increase in density leads to a decrease in a in a given time window [15]. The variation of $\langle r^2(t)\rangle$ in the α relaxation time scale also merge for both the cases.

V. DISCUSSION

The main thrust of this work is to present a comparison of the heterogeneous dynamics in the atomic (Newtonian) and the Brownian systems in the supercooled state. We present a detailed account of the computation of $\alpha_2(t)$ within the mode-coupling theory framework. The calculation of $\alpha_2(t)$ involves evaluating wave-vector integrals over the structural and self-correlation functions and the respective k derivatives. The present work illustrates the relevance of properly including the short wavelength fluctuations in such integrals, such that a convergence is obtained in the results. We found the existence of a double peak structure of the non-Gaussian parameter for both the systems following the Newtonian [15] and the stochastic dynamics. This is indicative of the characteristic two-step relaxation process of the correlation functions in dense liquid states. The computer simulation studies on charged colloidal liquids [12] in supercooled state reported such a *structured* variation of the non-Gaussian parameter. Qualitatively similar results from the molecular dynamics simulation of soft-sphere alloys were also reported in Ref. [38]. However, the computer simulation studies of the Lennard Jones binary mixtures in Ref. [8] show a smoothly rising single peak of the non-Gaussian parameter. In this case, $\alpha_2(t)$ increases during the β relaxation range and starts decaying towards zero in the α relaxation regime. The first peak as seen in our model for a one-component hard-sphere system is not observed there. These facts clearly point towards a need for a thorough probe in the shorter-time regimes. The short-time peak represents the effect of correlated dynamics in the shorter time scales. It is not observed if the mode-coupling effects in the dynamical equations are ignored. This short-time peak observed in our model occurs over the same time scale as observed in the kinetic theory models [16–18]. With the increase in density, correlated motions persist up to larger time scales and hence the second peak in $\alpha_2(t)$ has been generally observed in dense liquid state. This is observed both theoretically, as in our model, and in computer simulation studies [8,12].

In the present model, we find that the van Hove self-correlation function is a monotonically decreasing function for the colloidal systems (Fig. 9). However, in computer simulation of stochastic dynamics characterizing charged colloids, the probability $4\pi r^2 G_s(r,t)$ shows a two-peaked spatial variation [22]. This has been related to ''hopping'' processes [22] that restore ergodicity in the supercooled state. We do not observe the second peak in the corresponding result for the Brownian system. The present work is based on the theoretical model that includes the ergodicity restoring mechanisms only in the collective density dynamics [Eq. (3.6)] [26] and not in the tagged particle relaxation [Eq. (3.3) and (3.5)]. The inclusion of these in the theory will presumably produce more realistic results for the tagged particle dynamics. The comparison of $\alpha_2(t)$ obtained for the colloidal system in this model with the corresponding result of the light-scattering experiments [31] on the colloidal suspension shows that the longer-time peak in $\alpha_2(t)$ occurs on similar time scales. However, we find that the height of the peak is much shorter than that seen in experiment, implying that the type of relaxation is different quantitatively. No results in the shorter-time regime are reported in the experimental study [31]. A better comparison would be with the computer simulation studies done with the stochastic dynamics on hard-sphere systems comprising identical particles, where the higher-order properties such as $\alpha_2(t)$ are also evaluated.

ACKNOWLEDGMENTS

The authors acknowledge the Hahn Méitner Institüt, Berlin, for providing computational facilities. C.K. acknowledges financial support from the University Grants Commission, Council for Scientific and Industrial Research, India.

[1] M.T. Cicerone and M.D. Ediger, J. Chem. Phys. **104**, 7210 (1996).
[2] K. Schmidt-Rohr and H.W. Spiess, Phys. Rev. Lett. **66**, 3020 (1991); A. Heuer, M. Wilhelm, H. Zimmermann, and H.W. Spiess, *ibid.* **75**, 2851 (1995).
[3] R. Böhmer, G. Hinze, G. Diezemann, B. Geil, and H. Sillescu, Europhys. Lett. **36**, 55 (1996); **75**, 2851 (1995).
[4] A. Arbe, J. Colmenero, M. Monkenbusch, and D. Richter, Phys. Rev. Lett. **81**, 590 (1998).
[5] A. Heuer and H.W. Spiess, Phys. Rev. Lett. **82**, 1335 (1999).
[6] H. Silescu, J. Phys.: Condens. Matter **11**, A271 (1999).
[7] A. Rahman, Phys. Rev. **136**, A405 (1964).
[8] W. Kob, C. Donati, S. Plimpton, P.H. Poole, and S.C. Glotzer, Phys. Rev. Lett. **79**, 2827 (1997).
[9] C. Donati, J.F. Douglas, W. Kob, S.J. Plimpton, P.H. Poole, and S.C. Glotzer, Phys. Rev. Lett. **80**, 2338 (1998).
[10] B. Doliwa and A. Heuer, Phys. Rev. Lett. **80**, 4915 (1998).
[11] D. Caprion, J. Matsui, and H.R. Schober, Phys. Rev. Lett. **85**, 4293 (2000).
[12] S. Sanyal and A.K. Sood, Phys. Rev. E **57**, 908 (1998).
[13] R. Yamamoto and A. Onuki, Phys. Rev. Lett. **81**, 4915 (1998).
[14] S.C. Glotzer, V.M. Novikov, and T.B. Schroder, J. Chem. Phys. **112**, 509 (2000).
[15] C. Kaur and S.P. Das, Phys. Rev. Lett. **89**, 085701 (2002).

[16] M. Nelkin and A. Ghatak, Phys. Rev. **135**, A4 (1964).
[17] R.C. Desai and M. Nelkin, Nucl. Sci. Eng. **24**, 142 (1966).
[18] J.P. Boon and S. Yip, *Molecular Hydrodynamics* (Dover, New York, 1991).
[19] A.V. Indrani and S. Ramaswamy, Phys. Rev. Lett. **73**, 360 (1994).
[20] W. van Megen and P.N. Pusey, Phys. Rev. A **43**, 5429 (1991).
[21] W. van Megen, T.C. Mortensen, S.R. Williams, and J. Müller, Phys. Rev. E **58**, 6073 (1998).
[22] S. Sanyal and A.K. Sood, Europhys. Lett. **34**, 361 (1996).
[23] H. Löwen, J.P. Hansen, and J.N. Roux, Phys. Rev. A **44**, 1169 (1991).
[24] T. Gleim, W. Kob, and K. Binder, Phys. Rev. Lett. **81**, 4404 (1998).
[25] U. Bengtzelius, W. Götze, and A. Sjölander, J. Phys. C **17**, 5915 (1984).
[26] S.P. Das and G.F. Mazenko, Phys. Rev. A **34**, 2265 (1986).
[27] S.P. Das, Phys. Rev. A **36**, 211 (1987).
[28] T.R. Kirkpatrick and J.C. Nieuwoudt, Phys. Rev. A **33**, 2658 (1986).
[29] G. Szamel and H. Löwen, Phys. Rev. A **44**, 8215 (1991).
[30] G.F. Mazenko, S. Ramaswamy, and J. Toner, Phys. Rev. A **28**, 1618 (1983).
[31] T.C. Mortensen and W. van Megen, in *Slow Dynamics in Complex Systems*, edited by M. Tokuyama and I. Oppenheim, AIP Conf. Proc. No. 469 (AIP, Woodbury, NY, 1999), p. 3.
[32] S.P. Das, Phys. Rev. A **42**, 6116 (1990).
[33] L.V. Woodcock and C.A. Angell, Phys. Rev. Lett. **47**, 1129 (1981).
[34] S. Srivastava and S.P. Das, J. Chem. Phys. **116**, 2529 (2002).
[35] J. Yeo and G.F. Mazenko, J. Non-Cryst. Solids **172-174**, 1 (1994); Phys. Rev. E **51**, 5752 (1995).
[36] In the $t\rightarrow 0$ limit, the Eq. (3.3) reduces to a linearized form, from which $\psi_s(q,t)$ can be obtained in an analytical form. The cumulant expansion of this uptil $O(q^4)$ gives the $\alpha_2(t)$ whose $t\rightarrow 0$ limit is obtained as $-2/3$.
[37] M. Fuchs, W. Götze, and M.R. Mayr, Phys. Rev. E **58**, 3384 (1998).
[38] B. Bernu, J.P. Hansen, Y. Hiwatari, and G. Pastore, Phys. Rev. A **36**, 4891 (1987).